coatings

MDPI

Article

Preparation of Microcapsules of Urea Formaldehyde Resin Coated Waterborne Coatings and Their Effect on Properties of Wood Crackle Coating

Xiaoxing Yan [1,2,*] and Wenwen Peng [2]

[1] Co-Innovation Center of Efficient Processing and Utilization of Forest Resources, Nanjing Forestry University, Nanjing 210037, China
[2] College of Furnishings and Industrial Design, Nanjing Forestry University, Nanjing 210037, China; yjsww@njfu.edu.cn
* Correspondence: yanxiaoxing@nuaa.edu.cn

Received: 3 July 2020; Accepted: 1 August 2020; Published: 6 August 2020

Abstract: Urea formaldehyde coated waterborne acrylic resin microcapsules with core-wall ratios of 0.30, 0.45, 0.60, 0.67, and 0.75, and mass fractions of 1.0%, 4.0%, 7.0%, 10.0%, 13.0%, and 16.0% were prepared by in situ polymerization. Their micro morphology was examined by scanning electron microscope and infrared spectrum measurements. The gloss, color difference, adhesion, hardness, and impact resistance of the coating surface were investigated in detail. The influence of the core-wall ratio on the performance of the waterborne crackle coating on the wood surface and the self-healing performance were examined. The results showed that when the core-wall ratio of microcapsules was 0.67, an evenly dispersed powder state with particle size of about 3 μm microcapsules was obtained, and the highest coverage was achieved. When the mass fraction of the microcapsule was 4.0%, it had the optimum effect on surface performance. The adhesion was grade two, gloss was 10.9%, impact resistance was 15 kg·cm, chromatic aberration was 1.0, hardness was H, and it had the best effect on the healing of microcracks in the wood coating. As the coating added with microcapsules can inhibit the microcracks of the coating and plays a protective role for the substrate to achieve a self-healing effect, this study lays a technical foundation for the self-healing of surface cracks in coatings for wood.

Keywords: microcapsule; in-situ polymerization; waterborne crack coating; coating properties

1. Introduction

Using microcapsules has been described as an appropriate technique to release encapsulated material at targeted sites [1]. Microcapsule technology has been widely used in various fields such as medicine [2,3], textile [4], agriculture and animal husbandry [5,6], coatings [7], wood products [8,9] and furniture [10–12]. The encapsulated material can be solid, liquid, or gas, which plays a role in determining the function of microcapsules. The average particle size of microcapsules varies from 2 to 1000 μm [13]. Microcapsules can have various shapes, which are related to the coating materials. When the core material is liquid, microcapsules are spherical or elliptical. When the core of microcapsules are solid or crystal, their shape is irregular. Microencapsulation technology can be traced back to the 1930s [14]. Chen et al. [15] developed a novel multifunctional cellulose/silica hybrid microcapsule by one-step emulsion-solvent diffusion. These microcapsules were well dispersed into waterborne silicone resins to form waterborne multiple protective fabric coatings. Najjar et al. [16] reported the preparation and application of silica encapsulated isophorone diisocyanate (IPDI) as the active healing agent in the coatings fabricated by using waterborne polyurethane (WPU). Prepolymer method has been used to synthesize WPU, while IPDI-loaded silica capsules (SCS) were prepared via interfacial emulsion polymerization. Babaei et al. [17] prepared two kinds of reactive components with terminal azide and

propargyl functional groups embedded in tertiary amine atoms, which can repair the scratch area of the corrosion resistant coating. Patel et al. [18] prepared waterborne polyurethane dispersions (WBPUS) from phosphorous containing polyester polyol and isophorone diisocyanate. Li et al. [19] prepared graphene oxide microcapsules (GOMCS) with linseed oil as the curing agent by a self-assembly process. The corrosion resistance of GOMCS was improved, and the survival rate and surface wear resistance of GOMCS in a climate/marine environment was greatly improved. In our previous study [20], urea formaldehyde resin coated epoxy microcapsules were prepared by in situ polymerization and the optimal process parameters were explored. The self-healing effect was optimal when the core-wall ratio was 0.8:1, emulsifier concentration was 1%, stirring rate was 600 rpm, deposition time was 32 h, and mass fraction of the microcapsule was 10.0%.

Among environmental protection coatings, waterborne paint has a broad application prospect in the market because of its high safety, low cost and fast drying. Waterborne acrylic coatings have good impact resistance, abrasion resistance, scratch resistance, high hardness, and good adhesion. It also has excellent acid, alkali, and salt spray resistance [21]. Crack paint is a kind of art coating to make cracks appear on the surface of the coating for artistic effect. Urea formaldehyde resin has good physical and chemical properties, low cost, and can maintain the integrity of microcapsules without fracturing when coated. When the coating is damaged, the urea formaldehyde resin wall material can break easily and the microcapsules release the healing material [22].

In this paper, a waterborne acrylic coating was selected as the core material, and urea formaldehyde resin was used as the wall material of the microcapsule. The microcapsule was prepared by in situ polymerization [23–25]. Then, the prepared microcapsules were added into the waterborne crackle paint to prepare the coating. The self-healing effect, as well as the optical and mechanical properties of the coatings with the microcapsules were explored, and the appropriate amount of microcapsules and optimal parameters for the preparation of microcapsules were determined to provide a foundation for future research. Epoxy resin is a repair agent which needs high-temperature curing. The microcapsules prepared with waterborne acrylic coating as the core material are capable of room-temperature curing and crack self-healing, which are important characteristics for wood surface coatings. This can provide technical reference for self-healing waterborne wood coatings [26,27].

2. Materials and Methods

2.1. Experimental Materials

Formaldehyde solution (37.0%, M_w: 30.03 g/mol, CAS No.: 50-00-0), urea (M_w: 60.06 g/mol, CAS No.: 57-13-6) and triethanolamine (M_w: 149.19 g/mol, CAS No.: 102-71-6) were provided by Nanjing Chemical Reagent Co., Ltd., Nanjing, China. Benzyl alcohol (M_w: 108.13 g/mol, CAS No.: 100-51-6) and n-octanol (M_w: 130.23 g/mol, CAS No.: 111-87-5) were provided by Wuxi Yatai United Chemical Co., Ltd., Wuxi, China. Citric acid monohydrate (M_w: 210.14 g/mol, CAS No.: 5949-29-1) was provided by Tianjin Beilian Fine Chemicals Development Co., Ltd., Tianjin, China. Sodium dodecyl benzene sulfonate (M_w: 348.48 g/mol, CAS No.: 25155-30-0) was provided by Tianjin Beichen Fangzheng Reagent Factory, Tianjin, China. Waterborne acrylic coating used as core material was supplied by Nippon Paint Co., Ltd., Shanghai, China, which consisted of acrylic copolymers, dipropylene glycol methyl ether, and water. The mass fractions of acrylic copolymers, dipropylene glycol methyl ether, and water were 90.0%, 2.0%, and 8.0%, respectively. Waterborne crackle paint, mainly composed of waterborne polymer dispersion, was provided by Guangzhou Tianmai Chemical Technology Co., Ltd., Guangzhou, China. *Tilia europaea* boards (100 mm × 65 mm × 4 mm) were supplied by Yihua Lifestyle Technology Co., Ltd., Shantou, China.

2.2. Experimental Method

The wall material of this experiment was urea formaldehyde resin, and the core material was a waterborne acrylic coating. The reaction equation of urea and formaldehyde is

$$H_2N–CO–NH_2 + HCHO \rightarrow H–[NH–CO–NH–CH_2]–OH \quad (1)$$

According to Equation (1), the 30.0 g urea formaldehyde resin was obtained by the reaction of 20.0 g urea and 27.0 g formaldehyde solution with 37.0% concentration at molar mass of 1:1. The core-wall ratio is the mass ratio of the core material (waterborne acrylic coating) to the mass of the wall material (urea formaldehyde resin). The experimental raw materials were as follows (Table 1). First, the 20.0 g urea and 27.0 g formaldehyde solution with 37.0% concentration were mixed and stirred in a beaker; then, the triethanolamine was used to adjust the pH of the solution to 8.0–10.0. To obtain a slightly viscous and transparent urea formaldehyde pre-polymer solution, the magnetic stirrer was heated to 70 °C, rotating speed was set at 400 rpm, and the reaction time was 90 min. In addition, the 1.0% sodium dodecyl benzoate aqueous solution was prepared as an emulsifier. The waterborne acrylic coating was weighed and the benzyl alcohol as the diluent was added to the waterborne acrylic coating. The emulsifier and the diluent waterborne acrylic coatings were mixed and stirred at 1200 rpm, which reacted at 60 °C for 30 min, then several drops of n-octanol were added to defoamer and the core material emulsion was obtained. The urea formaldehyde prepolymer solution was slowly dripped into the core material emulsion. The citric acid was added to the above mixture to adjust the pH value to 2.0–3.0. Then, the reaction was continued for 3 h and the mixture was rinsed with deionized water and anhydrous ethanol many times. Then the solid was dried at 60 °C for 12 h, and the white microcapsule powder was obtained. The microcapsules were added into the waterborne crackle paint according at mass fractions of 1.0%, 4.0%, 7.0%, 10.0%, 13.0% and 16.0% and were coated on the *Tilia europaea* boards by SZQ tetrahedral fabricator (Senyuan Electric Co., Ltd., Zibo, China). The coated *Tilia europaea* boards were dried in the oven at 40 °C for 24 h. The dry coating thickness was about 60 μm.

Table 1. List of experimental raw materials.

Urea (g)	Formaldehyde Solution (g)	Urea Formaldehyde Resin (g)	Waterborne Acrylic Coating (g)	Sodium Dodecyl Benzene Sulfonate (g)	Deionized Water (g)	Core-Wall Ratio
20.0	27.0	30.0	9.0	0.70	69.30	0.30
20.0	27.0	30.0	13.5	1.04	102.96	0.45
20.0	27.0	30.0	18.0	1.39	137.61	0.60
20.0	27.0	30.0	20.0	1.54	154.44	0.67
20.0	27.0	30.0	22.5	1.76	174.24	0.75

2.3. Testing and Characterization

The color value of the crack paint coating on *Tilia europaea* boards surface was gauged with the SEGT-J Portable Colorimeter (Chugong Industry Co., Ltd., Shanghai, China). The "L" represents lightness, a large value means the surface color of the coating is bright and a small value means the color of the coating is dark. The "a" represents a change of color from red to green, a positive value indicates a reddish color and a negative value indicated a greenish color. The "b" represents a change of color from yellow to blue, with a positive value meaning the surface color of the measured object is yellowish, and a negative value meaning it is blueish. L_1, a_1 and b_1 are the chroma values of coating samples in a certain area, while L_2, a_2 and b_2 are the chroma values of coating samples in another area. ΔL (light difference) = $L_1 - L_2$, Δa (red-green difference) = $a_1 - a_2$, Δb (yellow-blue difference) = $b_1 - b_2$. The color difference was calculated according to Formula (2):

$$\Delta E = [(\Delta L)^2 + (\Delta a)^2 + (\Delta b)^2]^{1/2} \quad (2)$$

According to the standard "GB/T 4893.6-2013 test of surface coatings of furniture-Part 6: determination of gloss value" [28], the gloss of the paint film was gauged by an HG268 gloss

meter (3NH Technology Co., Ltd., Shenzhen, China). According to the standard "GB/T 6739-2006 paints and varnishes—determination of film hardness by pencil test" [29], the hardness of the film (determined by 6H, 5H, 4H, 3H, 2H, 1H, HB, 1B, 2B, 3B, 4B, 5B, and 6B pencils) was measured when scratches appeared on the coatings. The morphology of waterborne coatings was analyzed by Quanta 200 environmental scanning electron microscope (SEM), FEI Company (Hillsboro, OR, USA). The wall thickness of the microcapsules was analyzed using a L2800 biomicroscope (Guangzhou Liss Optical Instrument Co., Ltd., Guangzhou, China). The composition of the coating was analyzed by a vertex 80 V infrared spectrum analyzer (Germany Bruker Co., Ltd., Karlsruhe, Germany). The adhesion of the coating was determined by an QFH-HG600 adhesion tester (Shenzhen Sanenshi Technology Co., Ltd., Shenzhen, China). The impact resistance of paint film was measured by QCJ-50 impactor (Tianjin Jinghai Kexin testing machine factory, Tianjin, China). A cone hole with a top angle of 120° was drilled in the coating and the hole wall was imaged with a microscope magnified 40×. The coating part of the bus bar perpendicular to the microscope's main axis was read out. The length of the coating part of the bus was measured. According to the trigonometric function, the coating thickness is half of the length of the bus bar of coating part. The thickness of waterborne coating was calculated by three-point arithmetic method. The roughness of the paint films was measured by a JB-4C roughness meter (Shanghai Taiming Optical Instrument, Shanghai, China). All experiments were repeated four times with an error of less than 5.0%.

3. Results and Discussion

3.1. Microstructure Analysis

From Figure 1, it can be seen that the microcapsules with a core-wall ratio of 0.30 formed with complete spherical particles but the surface of the microcapsules was not smooth and there were some amorphous substances. The microcapsules with a core-wall ratio of 0.45 were not successfully coated; they were basically amorphous materials with a rough surface. Only a few formed microcapsules can be seen. The forming rate of microcapsules with a core-wall ratio of 0.60 was higher than the 0.45 core-wall ratio, but it was basically a mixture of mostly spherical particles and some with an amorphous state, and there were also large microcapsules. The microcapsules with a core-wall ratio of 0.67 were well-formed, with particle sizes of around 3 μm, and all of them were spherical, basically without rupture. The 0.67 core-wall ratio was the most suitable for microcapsules, and the shape and size of microcapsules were affected by the core-wall ratio, stirring speed, reaction temperature and time [30]. The microcapsules with a core-wall ratio of 0.75 were more spherical, although some were amorphous and broken.

With an electron microscope it can be observed that with core-wall ratios of 0.30, 0.67 and 0.75, microcapsules were well formed. Therefore, the infrared spectra of the three microcapsules were observed, as shown in Figure 2. At about 3300 cm^{-1} there was a wide and strong N-H absorption peak, which belongs to the characteristic functional group of urea formaldehyde resin. The absorption peak at 3000 cm^{-1} is characteristic of the C–H group, the absorption peak at 1650 cm^{-1} is characteristic of the C=O group, and the absorption peak at 1550 cm^{-1} is characteristic of the C–N group. These four absorption peaks correspond to the chemical bond in urea formaldehyde resin, indicating that urea formaldehyde resin had been synthesized in the system. In Figure 2, 1735 cm^{-1} represents the absorption peak of C=O in waterborne acrylic resin, 2950 cm^{-1} was the absorption peak of $–CH_3$, 2880 cm^{-1} was the absorption peak of $–CH_2–$, and 1250 cm^{-1} and 1150 cm^{-1} were the absorption peaks of C–O carboxyl group, indicating the presence of acrylic acid in the system. It can be concluded from the above infrared spectrum that there was urea formaldehyde resin and acrylic acid in the microcapsule sample. Figure 3 is a microscopic picture of the ruptured microcapsules, and the wall thickness of the microcapsules is about 1.1 μm. The acrylic acid was liquid, and if it is not the core material of the microcapsule, it would be filtered out. The acrylic acid was coated by urea formaldehyde resin, which indicated that the preparation of the microcapsule was successful. According to the analysis results of SEM and IR,

the microcapsules with core-wall ratios of 0.30, 0.67 and 0.75 were good. Therefore, microcapsules with core-wall ratios of 0.30, 0.67 and 0.75 were added to the waterborne crackle paint at the different mass fractions, and the effect of the core-wall ratio on the properties of crack paint was further studied.

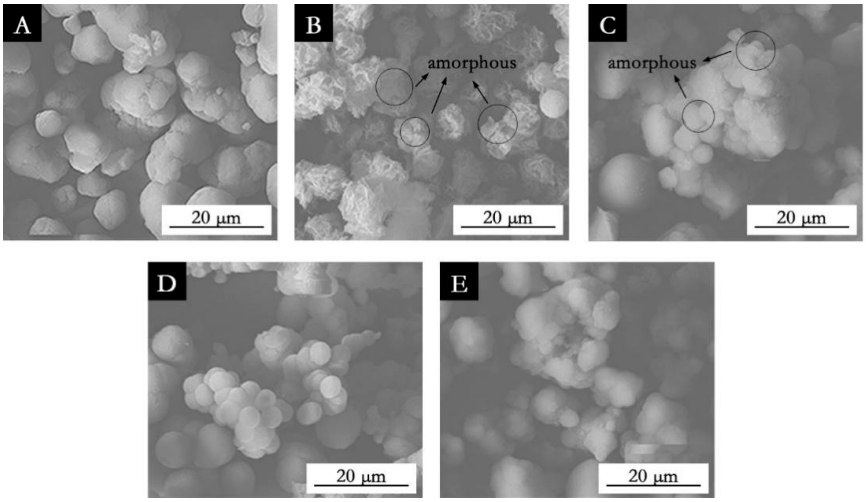

Figure 1. SEM of microcapsules with core-wall ratios of (**A**) 0.30, (**B**) 0.45, (**C**) 0.60, (**D**) 0.67, (**E**) 0.75.

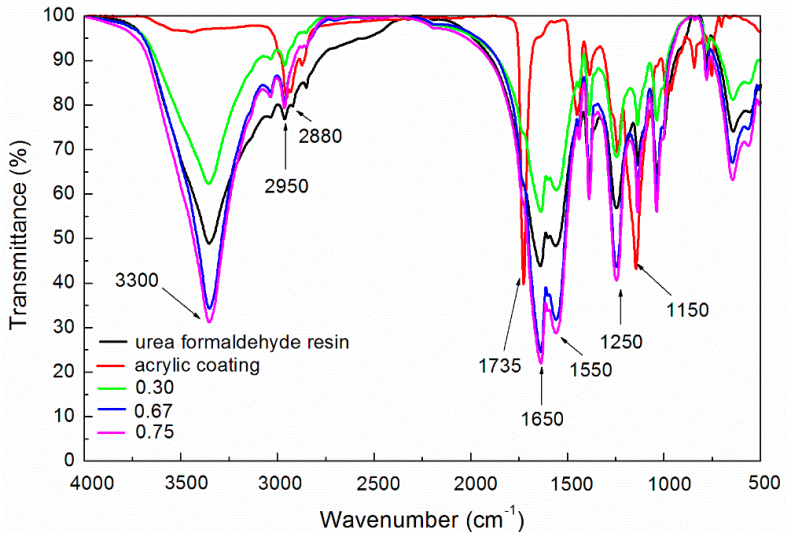

Figure 2. Infrared spectrum of microcapsules with different core-wall ratios.

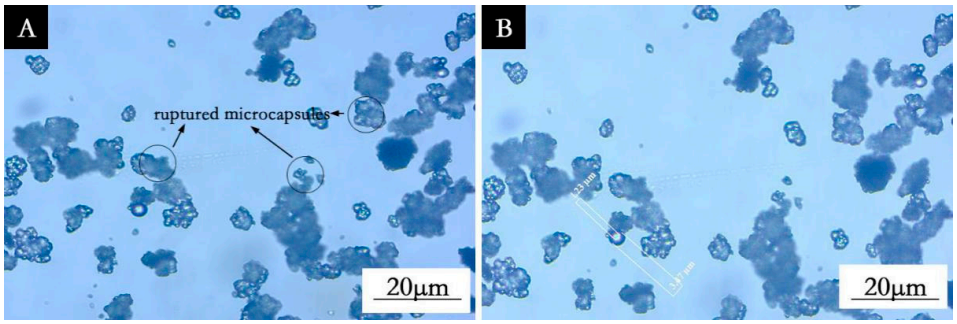

Figure 3. Microscopic picture of the ruptured microcapsules: (**A**) ruptured microcapsules, (**B**) the wall thickness of the microcapsules.

3.2. Effect of Different Core to Wall Ratio on the Gloss

Three kinds of gloss were measured at incident angles of 20°, 60° and 85°. The higher the value was, the higher the gloss was [31,32], which is shown in Table 2. It can be concluded that for microcapsules with the same core-wall ratio and incident angle, the gloss of the coating film without the microcapsules was the best, and then the gloss of the coating decreased with an increase of the mass fraction of the microcapsules. The reason for this is that an increase of microcapsules made the particles on the surface of the film increase, which led to an increase of diffuse reflection and decrease of gloss. With the incident angle held constant, when the core-wall ratio was 0.67, the surface gloss of the board was optimal, probably because the microcapsule powder was relatively fine. Gloss was optimal when the core-wall ratio of microcapsules was 0.67 and the mass fraction of microcapsules was 1.0–4.0%.

Table 2. Surface gloss of the crackle coating with microcapsules with different core-wall ratios.

Core-Wall Ratio	Microcapsule Mass Fraction (%)	20° (%)	60° (%)	85° (%)
-	-	4.1 ± 0.1	14.2 ± 0.4	22.8 ± 0.5
0.30	1.0	3.9 ± 0	11.0 ± 0.4	16.6 ± 0.5
0.30	4.0	3.7 ± 0	9.5 ± 0.2	4.1 ± 0.1
0.30	7.0	2.9 ± 0	5.5 ± 0.1	1.8 ± 0
0.30	10.0	2.4 ± 0	3.9 ± 0	0.7 ± 0
0.30	13.0	2.3 ± 0	3.2 ± 0.1	0.5 ± 0
0.30	16.0	1.9 ± 0	2.6 ± 0	0.3 ± 0
0.67	1.0	3.7 ± 0.1	11.0 ± 0.4	12.3 ± 0.4
0.67	4.0	3.5 ± 0.1	10.9 ± 0.3	8.7 ± 0.2
0.67	7.0	2.6 ± 0	4.6 ± 0.1	1.0 ± 0
0.67	10.0	2.4 ± 0	3.0 ± 0.1	0.2 ± 0
0.67	14.0	2.3 ± 0	2.4 ± 0	0.2 ± 0
0.67	16.0	2.3 ± 0	1.9 ± 0	0.2 ± 0
0.75	1.0	3.5 ± 0	10.4 ± 0.3	11.2 ± 0.2
0.75	4.0	3.1 ± 0	6.8 ± 0.2	5.6 ± 0.1
0.75	7.0	2.7 ± 0	5.6 ± 0.1	2.2 ± 0.1
0.75	10.0	2.5 ± 0	3.4 ± 0.1	0.8 ± 0
0.75	13.0	2.3 ± 0	3.3 ± 0.1	0.5 ± 0
0.75	16.0	2.2 ± 0	2.7 ± 0	0.3 ± 0

3.3. Effect of Different Core to Wall Ratio on the Adhesion

As shown in Table 3, level 1 indicates that there is no paint film falling off, level 2 indicates that there is paint film falling off at the intersection of cutting marks, level 3 indicates intermittent falling off along the cutting marks, level 4 indicates that there are large pieces peeling off in less than 50% of the cutting marks, and level 5 indicates that there are large pieces peeling off along the cutting marks in more than 50% of the squares. The results of adhesion on the coatings film surface are shown in Table 4. When the core-wall ratio was 0.30, the mass fraction of microcapsules increased from 0% to 20% and the coating film adhesion remained unchanged at the level 2. When the core-wall ratio was 0.67 and 0.75, the mass fraction of the microcapsules increased from 0% to 10% and the adhesion was level 2. When the mass fraction of microcapsules increased, adhesion reduced to level 3. When the core-wall ratio was 0.30, the adhesion did not change, which may be due to the fine powder and uniform coating. When the core-wall ratio was 0.67 and 0.75, the adhesion of the microcapsules decreased; this is because when the mass fraction of microcapsules is high, the particles agglomerate in the coating, which results in a decrease of the cohesion between the coating and the wood substrate [33]. When the mass fraction of microcapsules was less than 10%, there was no effect on surface adhesion.

Table 3. The adhesion grade of furniture surface coating.

Adhesion (Level)	Instruction
1	no paint film falling off
2	paint film falling off at the intersection of cutting marks
3	intermittent falling off along the cutting marks
4	large pieces peeling off in less than 50% of the cutting marks
5	large pieces peeling off along the cutting marks in more than 50% of the squares

Table 4. The adhesion of crackle paint with microcapsules that had different core-wall ratios.

Microcapsule Mass Fraction (%)	Adhesion (level)		
	0.30 Core-Wall Ratio	0.67 Core-Wall Ratio	0.75 Core-Wall Ratio
0	2 ± 0	2 ± 0	2 ± 0
1.0	2 ± 0	2 ± 0	2 ± 0
4.0	2 ± 0	2 ± 0	2 ± 0
7.0	2 ± 0	2 ± 0	2 ± 0
10.0	2 ± 0	2 ± 0	2 ± 0
13.0	2 ± 0	3 ± 0	3 ± 0
16.0	2 ± 0	3 ± 0	3 ± 0

3.4. Effect of Different Core to Wall Ratio on the Impact Resistance

It can be seen from Table 5 that when the mass fraction of microcapsules was the same, the impact resistance of the paint film with a core-wall ratio of 0.67 was better than those with core-wall ratios of 0.30 and 0.75. When the mass fraction of 0.67 core-wall ratio microcapsule was 4.0%, the impact resistance of the paint film was optimal. The addition of microcapsules affects the impact resistance of the film because the strength of urea formaldehyde resin is high, so it increases the impact resistance of the coating [34].

Table 5. Impact resistance of crackle paint finish with microcapsules with different core-wall ratios.

Microcapsule Mass Fraction (%)	Impact Resistance (kg·cm)		
	0.30 Core-Wall Ratio	0.67 Core-Wall Ratio	0.75 Core-Wall Ratio
0	13.0 ± 0.3	13.0 ± 0.4	13.0 ± 0.4
1.0	3.0 ± 0	9.0 ± 0	8.0 ± 0
4.0	5.0 ± 0	15.0 ± 0.4	9.0 ± 0.2
7.0	5.0 ± 0	13.0 ± 0.4	9.0 ± 0.2
10.0	7.0 ± 0.1	11.0 ± 0.3	10.0 ± 0
13.0	13.0 ± 0.3	12.0 ± 0.4	12.0 ± 0.4
16.0	13.0 ± 0.4	12.0 ± 0.4	12.0 ± 0.4

3.5. Effect of Different Core to Wall Ratio on the Hardness

From Table 6 it can be seen that with the addition of microcapsules, the hardness of the coating reduced, due to the fact that after the addition of microcapsules, it does not integrate with the paint as well, and the surface of the paint film is rougher (Table 7). The higher the mass fraction of microcapsules, the higher the roughness value. When microcapsules with the same mass fraction were added, using a mass fraction of 10% as an example, the microcapsules with 0.30 and 0.75 core-wall ratios had a surface hardness in the paint film of B, while microcapsules with a core-wall ratio of 0.67 had a surface hardness of the paint film of HB. The reason is that the microcapsules with a core wall ratio of 0.67 have good morphology and can fuse with the film interface better, enhancing the hardness [35,36]. When the mass fraction of microcapsules was the same, the surface hardness of the film was optimal at a core-wall ratio of 0.67.

Table 6. The hardness of crackle coating with microcapsules with different core-wall ratios.

Microcapsule Mass Fraction (%)	Hardness		
	0.30 Core-Wall Ratio	0.67 Core-Wall Ratio	0.75 Core-Wall Ratio
0	H ± 0	H ± 0	H ± 0
1.0	HB ± 0	H ± 0	H ± 0
4.0	HB ± 0	H ± 0	H ± 0
7.0	B ± 0	HB ± 0	HB ± 0
10.0	B ± 0	HB ± 0	B ± 0
13.0	B ± 0	B ± 0	B ± 0
16.0	2B ± 0	B ± 0	2B ± 0

Table 7. The surface roughness values of the coatings with microcapsules with different core-wall ratios.

Microcapsule Mass Fraction (%)	Surface Roughness (μm)		
	0.30 Core-Wall Ratio	0.67 Core-Wall Ratio	0.75 Core-Wall Ratio
0	0.4 ± 0	0.4 ± 0	0.4 ± 0
1.0	0.6 ± 0	0.5 ± 0	0.7 ± 0
4.0	5.5 ± 0.1	2.2 ± 0	4.2 ± 0.1
7.0	5.6 ± 0.1	4.9 ± 0.1	5.3 ± 0.1
10.0	5.7 ± 0.1	5.5 ± 0.1	5.7 ± 0.1
13.0	6.7 ± 0.1	6.5 ± 0.1	6.9 ± 0.1
16.0	8.0 ± 0.2	7.8 ± 0.1	8.3 ± 0.2

3.6. Effect of Different Core to Wall Ratios on Chromatic Aberration

Tables 8–10 show that when microcapsules with the same core-wall ratio were added, the chromatic aberration of the crack paint film on the surface of *Tilia europaea* boards increased with an increase of the mass fraction of microcapsules. With increased microcapsule mass fraction, the color difference increased from 0.7 to 2.8, 1.9 and 2.7 for microcapsules with a core-wall ratio of 0.30, 0.67 and 0.75, respectively. The results show that when the core-wall ratio was 0.67, the color difference of the microcapsules changed least, which was ideal.

Table 8. The color difference of coatings with microcapsules with a core-wall ratio of 0.30.

Mass Fraction of 0.30 Core-Wall Ratio Microcapsule (%)	L_1	a_1	b_1	L_2	a_2	b_2	△E
0	21.8 ± 0.6	2.0 ± 0	8.8 ± 0.2	22.3 ± 0.5	2.0 ± 0	8.4 ± 0	0.7 ± 0
1.0	24.2 ± 0.7	0.2 ± 0	8.7 ± 0.1	23.7 ± 0.3	0.8 ± 0	7.5 ± 0.2	1.5 ± 0
4.0	30.4 ± 0.7	1.0 ± 0	9.8 ± 0.3	31.3 ± 0.5	0.4 ± 0	8.8 ± 0.2	1.6 ± 0
7.0	24.2 ± 0.6	0.2 ± 0	8.7 ± 0.3	23.1 ± 0.6	0.1 ± 0	7.7 ± 0.2	1.6 ± 0
10.0	23.0 ± 0.7	0.1 ± 0	9.6 ± 0.2	23.6 ± 0.2	−0.6 ± 0	11.0 ± 0.7	1.7 ± 0
13.0	26.0 ± 0.5	0.5 ± 0	9.5 ± 0.3	26.3 ± 0.5	−0.9 ± 0	10.4 ± 0.3	1.8 ± 0
16.0	24.6 ± 0.5	1.0 ± 0	6.4 ± 0.2	22.6 ± 0.7	1.3 ± 0	4.5 ± 0.1	2.8 ± 0

Table 9. The color difference of coatings with microcapsules with a core-wall ratio of 0.67.

Mass Fraction of 0.67 Core-Wall Ratio Microcapsule (%)	L_1	a_1	b_1	L_2	a_2	b_2	△E
0	21.8 ± 0.6	2.0 ± 0	8.8 ± 0.2	22.3 ± 0.5	2.0 ± 0	8.4 ± 0	0.7 ± 0
1.0	24.4 ± 0.5	2.2 ± 0	9.1 ± 0.2	24.4 ± 0.4	3.0 ± 0	9.2 ± 0.2	0.8 ± 0
4.0	25.7 ± 0.5	2.3 ± 0	10.4 ± 0.3	25.9 ± 0.7	1.5 ± 0	9.8 ± 0.2	1.0 ± 0
7.0	24.3 ± 0.7	1.2 ± 0	8.9 ± 0.2	22.9 ± 0.8	1.7 ± 0	8.5 ± 0.3	1.6 ± 0
10.0	23.2 ± 0.5	1.2 ± 0	9.9 ± 0.2	21.7 ± 0.2	1.8 ± 0	9.6 ± 0.2	1.7 ± 0
13.0	24.3 ± 0.7	1.2 ± 0	8.9 ± 0.2	24.3 ± 0.6	1.8 ± 0	7.2 ± 0.2	1.8 ± 0
16.0	24.4 ± 0.5	2.2 ± 0	9.1 ± 0.2	22.6 ± 0.8	2.8 ± 0	9.1 ± 0.2	1.9 ± 0

Table 10. The color difference of coatings with microcapsules with a core-wall ratio of 0.75.

Mass Fraction of 0.75 Core-Wall Ratio Microcapsule (%)	L_1	a_1	b_1	L_2	a_2	b_2	△E
0	21.8 ± 0.6	2.0 ± 0	8.8 ± 0.2	22.3 ± 0.5	2.0 ± 0	8.4 ± 0	0.7 ± 0
1.0	26.8 ± 0.6	1.6 ± 0	11.2 ± 0.6	27.0 ± 0.8	2.4 ± 0	13.0 ± 0.4	2.0 ± 0
4.0	21.7 ± 0.6	−1.0 ± 0	10.5 ± 0.3	20.0 ± 0.2	−2.0 ± 0	11.7 ± 0.5	2.3 ± 0
7.0	26.2 ± 0.9	2.3 ± 0	9.9 ± 0.2	25.5 ± 0.4	1.8 ± 0	12.0 ± 0.2	2.3 ± 0
10.0	24.4 ± 0.5	2.2 ± 0	9.1 ± 0.2	26.2 ± 0.9	3.2 ± 0.1	10.0 ± 0.2	2.4 ± 0
13.0	24.9 ± 0.4	2.1 ± 0	8.7 ± 0.3	24.7 ± 0.5	4.4 ± 0	7.9 ± 0.1	2.5 ± 0
16.0	23.6 ± 0.6	0.2 ± 0	9.1 ± 0.3	24.4 ± 0.4	−2.3 ± 0	9.5 ± 0.2	2.7 ± 0

3.7. Self Repair Test

From the above analysis, it can be seen that the coating with a core-wall ratio of 0.67 exhibited least chromatic aberration and better mechanical properties. Therefore, the effect of microcapsules with a core-wall ratio of 0.67 on the coating repair performance was studied. Figure 4 shows the SEM of the coating with microcapsules with different mass fractions. When the mass fraction of microcapsules was 0, the surface of the coating was smooth and even, and only the cracks in the coating surface can be seen. When the mass fraction of microcapsules was 4.0%, the surface of the coating was very smooth. When the mass fraction of microcapsules was increased to 13.0%, there was an obvious phenomenon of aggregation of microcapsules on the surface. It can be seen that when the mass fraction of microcapsules was relatively low, it had little effect on the surface of the coating. When the mass fraction of microcapsules increased further, microcapsules were not easy to disperse and agglomerated in the coating easily.

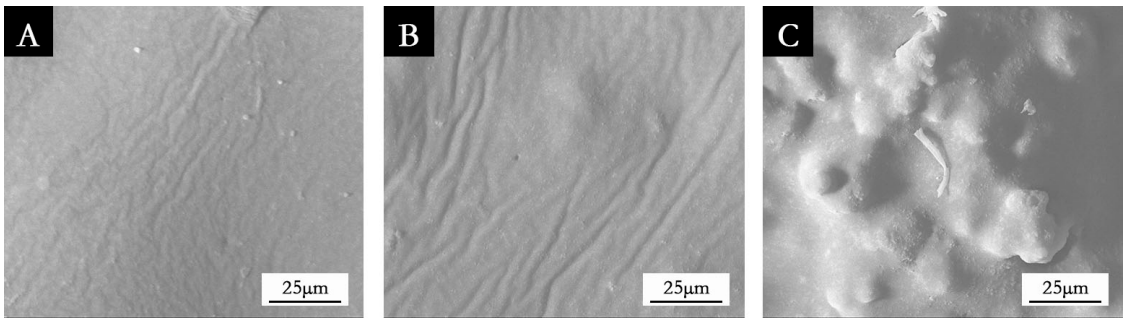

Figure 4. SEM picture of the coating under different mass fractions of microcapsule: (**A**) 0%, (**B**) 4.0%, (**C**) 13.0%.

As can be seen in Figure 5, when the crack paint did not have added microcapsules, the cracking is obvious. After adding microcapsules with different mass fractions, the healing function of cracks is preliminarily shown. When the mass fraction of microcapsules was 1.0% and 4.0%, the healing function is most obvious, and only slight cracks can be seen with the naked eye. When the mass fraction of microcapsules was 7.0%, cracks appeared again. When the mass fraction was over 10.0%, it can be seen that the microcapsules accumulated on the surface of the crackle coatings without the self-healing effect.

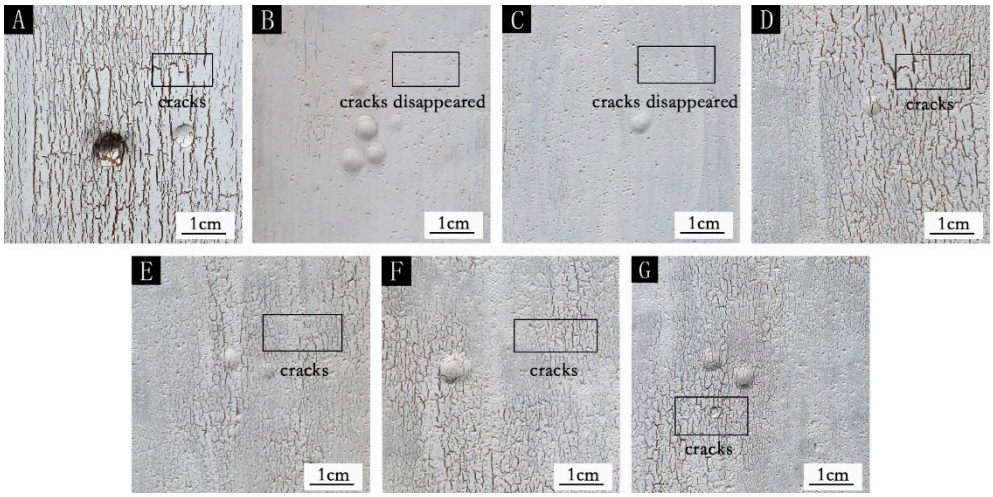

Figure 5. Self-healing effect of different mass fraction of microcapsules with crack coating: (**A**) 0%, (**B**) 1.0%, (**C**) 4.0%, (**D**) 7.0%, (**E**) 10.0%, (**F**) 13.0%, (**G**) 16.0%.

4. Conclusions

This study fabricated a preparation method for urea formaldehyde resin coated waterborne coating microcapsules by in situ polymerization and revealed its effect on properties of wood crackle coating in detail. Different core-wall ratios were examined. Based on SEM images, when the core-wall ratio was 0.67, the roundest and most spherical shape of microcapsules was obtained, there were less broken microcapsules and they were free from impurities. When the mass fraction of microcapsules with a core-wall ratio of 0.67 was 4.0% in the crackle paint finish, the coating gloss decreased slightly, chromatic aberration reduced, adhesion and hardness did not change, and the repair effect was better. These results provide a technical basis for the application of microcapsules in the self-repair of coatings.

Author Contributions: Conceptualization, X.Y.; Methodology, X.Y.; Validation, X.Y.; Resources, X.Y.; Data Curation, X.Y.; Writing—Original Draft Preparation, X.Y.; Supervision, X.Y.; Data Analysis, W.P.; Investigation, W.P.; Writing—Review and Editing, W.P. All authors have read and agreed to the published version of the manuscript.

Funding: This project was partly supported by the General Program of Jiangsu Natural Science Foundation in 2020 (Project title: Study on the relationship between microstructure control of self repairing coating and wood based on microcapsule technology) and the Youth Science and Technology Innovation Fund of Nanjing Forestry University, Grant Number (CX2016018).

Conflicts of Interest: The authors declare no conflict of interest.

References

1. Solomando, J.C.; Antequera, T.; Perez-Palacios, T. Lipid digestion and oxidative stability in omega-3-enriched meat model systems: Effect of fish oil microcapsules and processing or culinary cooking. *Food Chem.* **2020**, *328*, 127125. [CrossRef] [PubMed]
2. Du, W.; Yu, J.Y.; Gu, S.J.; Wang, R.Y.; Li, J.T.; Han, X.B.; Liu, Q.T. Effect of temperatures on self-healing capabilities of concrete with different shell composition microcapsules containing toluene-di-isocyanate. *Constr. Build. Mater.* **2020**, *247*, 118575. [CrossRef]
3. Mou, C.L.; Deng, Q.Z.; Hu, J.X.; Wang, L.Y.; Deng, H.B.; Xiao, G.Q.; Zhan, Y.Q. Controllable preparation of monodisperse alginate microcapsules with oil cores. *J. Colloid Interface Sci.* **2020**, *569*, 307–319. [CrossRef] [PubMed]
4. Li, J.; Zhang, Y.T.; Zhang, Z.B.; Liu, H.L.; Rui, J.M.; Li, Y.J.; Chen, Z. Preparation of phase change microcapsules-aerogels composites and the enhanced thermal properties. *Mater. Lett.* **2020**, *268*, 127563. [CrossRef]
5. Wang, S.J.; Shi, Y.; Han, L.P. Development and evaluation of microencapsulated peony seed oil prepared by spray drying: Oxidative stability and its release behavior during in-vitro digestion. *J. Food. Eng.* **2018**, *231*, 1–9. [CrossRef]

6. Uzoma, P.C.; Liu, F.C.; Han, E.H. Multi-stimuli-triggered and self-repairable fluorocarbon organic coatings with urea-formaldehyde microcapsules filled with fluorosilane. *J. Mater. Sci. Technol.* **2020**, *45*, 70–83. [CrossRef]
7. Xu, W.; Fang, X.Y.; Han, J.T.; Wu, Z.H.; Zhang, J.L. Effect of coating thickness on sound absorption property of four wood species commonly used for piano soundboards. *Wood Fiber Sci.* **2020**, *52*, 28–43. [CrossRef]
8. Fang, L.; Xiong, X.Q.; Wang, X.H.; Chen, H.; Mo, X.F. Effects of surface modification methods on mechanical and interfacial properties of high-density polyethylene-bonded wood veneer composites. *J. Wood Sci.* **2017**, *63*, 65–73. [CrossRef]
9. Xiong, X.Q.; Ma, Q.R.; Yuan, Y.Y.; Wu, Z.H.; Zhang, M. Current situation and key manufacturing considerations of green furniture in China: A review. *J. Clean. Prod.* **2020**, *267*, 121957. [CrossRef]
10. Ebrahimnezhad-Khaljiri, H.; Eslami-Farsani, R. The tensile properties and interlaminar shear strength of microcapsules-glass fibers/epoxy self-healable composites. *Eng. Fract. Mech.* **2020**, *230*, 106937. [CrossRef]
11. Wurth, R.; Foerst, P.; Kulozik, U. Effects of skim milk concentrate dry matter and spray drying air temperature on formation of capsules with varying particle size and the survival microbial cultures in a microcapsule matrix. *Dry. Technol.* **2018**, *36*, 93–99. [CrossRef]
12. Han, S.J.; Chen, Y.P.; Lyu, S.Y.; Chen, Z.L.; Wang, S.Q.; Fu, F. Effects of processing conditions on the properties of paraffin/melamine-urea-formaldehyde microcapsules prepared by in situ polymerization. *Colloids Surf. A* **2020**, *585*, 124046. [CrossRef]
13. Wei, J.; Ju, X.J.; Xie, R.; Mou, C.L.; Lin, X.; Chu, L.Y. Novel cationic pH-responsive poly (N,N-dimethylaminoethyl methacrylate) microcapsules prepared by a microfluidic technique. *J. Colloid Interface Sci.* **2011**, *357*, 101–108. [CrossRef] [PubMed]
14. Wu, S.M.; Li, Y.; Gu, A.J.; Liang, G.Z. Synthesis and characterization of novel epoxy resins-filled microcapsules with organic/inorganic hybrid shell for the self-healing of high performance resins. *Polym. Advan. Technol.* **2016**, *27*, 1544–1556. [CrossRef]
15. Chen, K.L.; Zhou, J.L.; Che, X.G.; Zhao, R.Y.; Gao, Q. One-step synthesis of core shell cellulose-silica/n-octadecane microcapsules and their application in waterborne self-healing multiple protective fabric coatings. *J. Colloid Interface Sci.* **2020**, *566*, 401–410. [CrossRef]
16. Najjar, R.; Akbari, M.; Mirmohseni, A.; Hosseini, M. Preparation and corrosion performance of healable waterborne polyurethane coatings containing isophoronediisocyanate loaded silica capsules. *J. Taiwan Inst. Chem. Eng.* **2018**, *93*, 1–10. [CrossRef]
17. Babaei, N.; Yeganeh, H.; Gharibi, R. Anticorrosive and self-healing waterborne poly(urethane-triazole) coatings made through a combination of click polymerization and cathodic electrophoretic deposition. *Eur. Polym. J.* **2019**, *112*, 636–647. [CrossRef]
18. Patel, R.H.; Kapatel, P.M. Studies on the effect of the size of waterborne polyurethane nanoparticles on properties and performance of coatings. *Int. J. Polym. Anal. Charact.* **2019**, *24*, 1–9. [CrossRef]
19. Li, J.; Feng, Q.K.; Cui, J.C.; Yuan, Q.Q.; Qiu, H.X.; Gao, S.L.; Yang, J.H. Self-assembled graphene oxide microcapsules in pickering emulsions for self-healing waterborne polyurethane coatings. *Compos. Sci. Technol.* **2017**, *151*, 282–290. [CrossRef]
20. Yan, X.X.; Chang, Y.J.; Qian, X.Y. Preparation and self-repairing properties of urea formaldehyde-coated epoxy resin microcapsules. *Int. J. Polym. Sci.* **2019**, *2019*, 7215783. [CrossRef]
21. Khanjani, J.; Hanifpour, A.; Pazokifard, S.; Zohuriaan-Mehr, M.J. Waterborne acrylic-styrene/PDMS coatings formulated by different particle sizes of PDMS emulsions for outdoor applications. *Prog. Org. Coat.* **2020**, *141*, 105267. [CrossRef]
22. Tzavidi, S.; Zotiadis, C.; Porfyris, A.; Korres, D.M.; Vouyiouka, S. Epoxy loaded poly(urea-formaldehyde) microcapsules via in situ polymerization designated for self-healing coatings. *J. Appl. Polym. Sci.* **2020**, e49323. [CrossRef]
23. Cotting, F.; Koebsch, A.; Aoki, I.V. Epoxy self-healing coating by encapsulated epoxy ester resin in poly (urea-formaldehyde-melamine) microcapsules. *Front. Mater.* **2019**, *6*, 314. [CrossRef]
24. Wang, Y.Y.; Li, Y.D.; Zhang, Z.X.; Zhao, H.S.; Zhang, Y.F. Repair performance of self-healing microcapsule/epoxy resin insulatig composite to physical damage. *Appl. Sci.* **2019**, *9*, 4098. [CrossRef]
25. Zhu, H.Y.; Zhang, M.L.; Zhang, S.M. Preparation of macroporous polymers from microcapsule-stabilized pickering high internal phase emulsions. *Langmuir* **2019**, *35*, 9504–9512. [CrossRef]

26. Fan, W.J.; Zhang, Y.; Li, W.H.; Wang, W.; Zhao, X.D.; Song, L.Y. Multi-level self-healing ability of shape memory polyurethane coating with microcapsules by induction heating. *Chem. Eng. J.* **2019**, *368*, 1033–1044. [CrossRef]
27. Yan, X.X.; Wang, L.; Qian, X.Y. Effect of urea-formaldehyde-coated epoxy microcapsule modification on gloss, toughness and chromatic distortion of acrylic copolymers waterborne coating. *Coatings* **2019**, *9*, 239. [CrossRef]
28. GB/T 4893.6-2013. *Test of Surface Coatings of Furniture—Part 6: Determination of Gloss Value*; Standardization Administration of the People's Republic of China: Beijing, China, 2013; pp. 1–6. (In Chinese)
29. GB/T 6739-2006. *Paints and Varnishes—Determination of Film Hardness by Pencil Test*; Standardization Administration of the People's Republic of China: Beijing, China, 2006; pp. 1–5. (In Chinese)
30. Xu, D.S.; Chen, W.; Fan, X.C. Experimental investigation of particle size effect on the self-healing performance of microcapsule for cemented coral sand. *Constr. Build. Mater.* **2020**, *256*, 119343. [CrossRef]
31. Li, Y.; Wang, G.Q.; Guo, Z.H.; Wang, P.Q.; Wang, A.M. Preparation of microcapsules coating and the study of their bionic anti-fouling performance. *Materials* **2020**, *13*, 1669. [CrossRef]
32. Yao, J.L.; Yang, C.P.; Zhu, C.F.; Hou, B.Q. Preparation process of epoxy resin microcapsules for self—Healing coatings. *Prog. Org. Coat.* **2019**, *132*, 440–444.
33. Katoueizadeh, E.; Zebarjad, S.M.; Janghorban, K. Morphological study of surface-modified urea-formaldehyde microcapsules using 3-aminopropyltriethoxy silane. *Polym. Bull.* **2019**, *76*, 1317–1331. [CrossRef]
34. Yan, X.X.; Qian, X.Y.; Chang, Y.J. Preparation and characterization of urea formaldehyde @ epoxy resin microcapsule on waterborne wood coatings. *Coatings* **2019**, *9*, 475. [CrossRef]
35. Hou, J.H.; Peng, Z.G.; Feng, Q. Synthesis and properties of microencapsulated phase change material with a urea-formaldehyde resin shell and paraffin wax core. *J. Appl. Polym. Sci.* **2019**, *137*, 48578.
36. Zheng, N.; Qiao, L.; Liu, J.; Li, W.G.; Li, C.M.; Liu, Q.; Xue, Y.; Zhang, Q.Y. Microcapsules of multilayered shell structure synthesized via one-part strategy and their application in self-healing coatings. *Compos. Commun.* **2019**, *12*, 26–32. [CrossRef]